Charge-Carrier Evolution in Electrically Conducting Substituted Polymers Containing Biheterocycle/*p*-Phenylene Repeat Units

Andrew D. Child,[1] Balasubramanian Sankaran, Fernando Larmat, and John R. Reynolds*

Center for Macromolecular Science and Engineering, Department of Chemistry, University of Florida, Gainesville, Florida 32611

Received April 4, 1995[⊗]

ABSTRACT: The effects of backbone and pendant side-chain structure on the electronic and electrochemical properties of a series of poly[1,4-bis(2-heterocycle)-*p*-phenylenes] have been studied using a combination of optical spectroscopic, electrochemical, and EPR techniques. The selection of the heterocycle (thiophene or furan) and the nature of the pendant groups, substituted at the 2 and 5 positions of the phenyl ring, were found to impart a strong influence on the types and stability of electrochemically created charge carriers. Substitution with long-chain alkoxy substituents results in a decrease in the monomer and polymer oxidation potentials, narrowing of the electronic bandgap relative to unsubstituted or alkyl-substituted derivatives, and the creation of metallic charge carriers at the highest doping levels. Two oxidation states can be clearly resolved in the cyclic voltammograms of these alkoxy derivatives indicating the formation of stable, polaron species at intermediate doping levels. The synthesis of a new monomer, 1,4-bis(2-thienyl)-2,5-bis[(cyclohexylmethyl)oxy]benzene, and its polymer prepared using both chemically and electrochemically induced oxidative polymerization methods are reported. This monomer displays unique electropolymerization behavior with two oxidative redox processes during electrochemical polymerization. The first redox process (onset ca. +0.65 V vs Ag/Ag^+) results in exceedingly slow film growth. Polymer film growth at the second oxidation (onset ca. +0.9 V vs Ag/Ag^+) is ca. 25 times more rapid.

Introduction

The structural modification of conjugated polymers, by the attachment of flexible substituents, has proved effective in introducing solubility and fusibility to intrinsically insoluble and intractable backbones. As examples, soluble derivatives of polythiophene,[2] polypyrrole[3] and poly(*p*-phenylene)[4] have been reported. Substitution with sufficiently long alkyl chains has led to the preparation of true thermoplastic materials which can be processed using both solution and melt methods. When the substituents are ionic in nature, conjugated polyelectrolytes are formed which can be water soluble.[5]

In addition to the inducement of processability, the substitution of conjugated polymers has been shown to exert a strong influence on their optical, electrical, and electrochemical properties. We[6] and others[7] have been probing these effects in studies of the poly[1,4-bis(2-heterocycle)-*p*-phenylenes] (PBHPs), as outlined by structures **P1**–**P11**, which provide a large number of

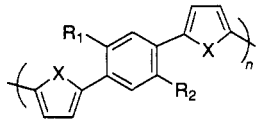

X = S	X = O
P1: $R_1 = R_2 = H$	**P7**: $R_1 = R_2 = H$
P2: $R_1 = R_2 = CH_3$	**P8**: $R_1 = R_2 = CH_3$
P3: $R_1 = R_2 = OCH_3$	**P9**: $R_1 = R_2 = OCH_3$
P4: $R_1 = OCH_3$, $R_2 = OC_7H_{15}$	**P10**: $R_1 = OCH_3$, $R_2 = OC_7H_{15}$
P5: $R_1 = R_2 = OC_7H_{15}$	**P11**: $R_1 = R_2 = OC_7H_{15}$
P6: $R_1 = R_2 =$ 	

derivatives by changing both the backbones and substituents. The electron-donating nature of alkoxy substituents has been shown to lower monomer and polymer oxidation potentials and reduce the optical bandgap by increasing the electron density in π-conjugated systems.

Pendant substituents have also been shown to have a strong steric influence on the conformation of the conjugated backbone. Steric repulsions between substituents on adjacent rings results in an increase in the energy barrier to attaining a planar π system.[8] Since planarity is desired for charge-carrier stabilization and transport, this torsional strain leads to an increase in oxidation potentials and a decrease in electrical conductivity. This effect is demonstrated by poly[1,4-bis-(2-thienyl)-2,5-dimethylphenylene] (**P2**), where the thiophene–phenylene torsional angle has been calculated to be significantly larger than either the unsubstituted or dimethoxy (**P3**) analogues.[6a] More importantly, the energy barrier to ring planarity increases from 3.1 to 15.8 kcal/mol with methyl substitution. This results in an increase in both the monomer and polymer oxidation potentials and a decrease in conductivity of more than 5 orders of magnitude.

Our studies of the PBHPs were initially motivated by the potential for soluble *p*-phenylene-containing polymers which would exhibit the desirable electronic properties of the polyheterocycles. Due to the ease of substitution on the phenylene ring, the synthesis of a large number of derivatives has been made possible. The fact that the monomers can be symmetrically derivatized to yield isoregic polymers with enhanced order and, in some cases, liquid crystallinity is an additional benefit of these polymers.[6b] It is generally accepted that higher degrees of long-range order can lead to significant enhancements in electrical conductivity.

In the PBHPs, we have found that while the parent polyheterocycle properties are largely retained, some unique electrochemical phenomena are observed in both monomers during electropolymerization and polymers during redox switching. This paper reports a new derivative in this series containing cyclic alkoxy pen-

[⊗] Abstract published in *Advance ACS Abstracts,* August 1, 1995.

0024-9297/95/2228-6571$09.00/0

dants, poly[1,4-bis(2-thienyl)-2,5-bis[(cyclohexylmethyl)oxy]phenylene] (**P6**), which displays two oxidations in the cyclic voltammogram of its *monomer*. In this instance, electropolymerization and conducting polymer film deposition are retarded during the first redox process and rapidly accelerated during the second. The thiophene[6c] and furan[6d] polymer derivatives, substituted with long-chain alkoxy substituents, display some unique electrochemical behavior as well. The cyclic voltammograms reveal a separation of the neutral-to-polaron and polaron-to-bipolaron redox events which is not observed in the unsubstituted or alkyl-substituted PBHP derivatives. This behavior has been observed in a variety of alkoxy-[9] and alkyl-[10]substituted polythiophenes, as well as oligomeric thiophene species,[11] and has been attributed to counterion complexation,[9d] π-hexamer dimerization,[11] and the stabilization of polaron intermediates.[9a,10] In this paper, we examine the stability and concentration of these paramagnetic intermediate charge carriers using in situ EPR/electrochemistry. In addition, utilizing optoelectrochemistry, metallic charge carriers are observed at high doping levels in poly-[1,4-bis(2-thienyl)-2,5-bis[(cyclohexylmethyl)oxy]phenylene] (**P6**). The presence and concentration of paramagnetic charge carriers at intermediate doping levels (polarons) and metallic charge carriers at high potentials indicate the importance of morphology and steric effects on the electronic properties of the polymer.

Experimental Section

Materials and Methods. Cyclohexylmethyl bromide, hydroquinone, bromine, KOH, 2-thienyllithium, zinc chloride, and palladium tetrakistriphenylphosphine were used as received (Aldrich). Monomers were prepared as reported previously.[6] All solvents were freshly dry distilled before use. All reactions were carried out under an argon atmosphere with specific care being taken in handling of the palladium catalyst and anhydrous zinc chloride. Characterization was carried out using ^{1}H and ^{13}C NMR spectroscopy on Varian XL-200 and Varian XL-300 spectrometers, FTIR on a Biorad/Digilab FTS-40 spectrophotometer, and mass spectrometry on a Finnigan MAT 95 Q spectrometer. Elemental analysis was carried out by Atlantic Microlab Inc.

1,4-Bis[(cyclohexylmethyl)oxy]benzene. Alcoholic KOH (14.5 g, 258 mmol) was added slowly to hydroquinone (13.5 g, 123 mmol) in 100 mL of ethanol. The reaction mixture was stirred for 2 h, and 50 g (282 mmol) of cyclohexylmethyl bromide in 50 mL of ethanol was added dropwise over 30 min. The mixture was refluxed for 48 h, and the ethanol removed. The residue was extracted with CCl_4, dried over $CaCl_2$, and filtered. The solution was evaporated to dryness and white flaky crystals were obtained after recrystallization from ethanol (mp = 93−95 °C, 41%). Mass spectrometry: molecular ion peak, 302.2 amu; base peak, 206.1 amu.

1,4-Dibromo-2,5-bis[(cyclohexylmethyl)oxy]benzene. Bromine (76 mmol) in 100 mL of CCl_4 was added dropwise to a 150 mL CCl_4 solution of 1,4-bis[(cyclohexylmethyl)oxy]-benzene (25.4 mmol). The reaction mixture was stirred for 72 h, poured into 150 mL of 1.0 M KOH, and stirred for an additional 2 h. The aqueous layer was discarded and the organic layer washed with dilute HCl until the pH reached 7.0. The solution was concentrated by evaporation and poured slowly into cold methanol. The precipitate was collected by filtration, dried and recrystallized from ethyl acetate to give a white solid (mp = 130−132 °C, 89%). ^{1}H NMR (ppm) 7.05-(s), 3.73(d), 1−2(m). ^{13}C NMR (ppm) 150.2, 111.4, 111.1, 75.6, 37.7, 29.8, 26.5, 25.8. Anal. Calcd for $C_{20}H_{28}O_2Br_2$: C, 52.19; H, 6.13. Found: C, 51.95; H, 6.13.

1,4-Bis(2-thienyl)-2,5-bis[(cyclohexylmethyl)oxy]benzene (6). 2-Thienyllithium (35.7 mmol) was added slowly with stirring at 0 °C to a flask containing zinc chloride (64.3 mmol) in 100 mL of THF. In a separate flask, 1,4-Dibromo-2,5-bis-[(cyclohexylmethyl)oxy]benzene (11.9 mmol) in 100 mL of THF was added to 50 mg of palladium tetrakistriphenylphosphine via cannula at 0 °C over 30 min. The 2-thienylzinc chloride was cannulated into the flask containing the 1,4-dibromo-2,5-bis[(cyclohexylmethyl)oxy]benzene and the mixture stirred for 72 h at 0 °C. The mixture was poured into 100 mL of dilute HCl, and the organic layer separated. The aqueous layer was extracted with ether and the ether fractions combined. The product was precipitated into cold methanol and recrystallized from acetone to yield a greenish solid (mp = 162−164 °C, 82%). ^{1}H NMR (ppm) 7.52 (dd), 7.33 (dd), 7.11 (dd), 3.8 (d), 1−2 (m). ^{13}C NMR (ppm) 149.3, 139.3, 126.6, 125.6, 125.1, 122.9, 112.8, 75.3, 37.9, 30.1, 26.5, 25.9. Anal. Calcd for $C_{28}H_{34}O_2S_2$: C, 72.06; H, 7.34; S, 13.74. Found: C, 71.98; H, 7.42; S, 13.56. Mass spectrometry: molecular ion peak, 466.2 amu; base peak, 274.0 amu.

Chemically Prepared Poly[1,4-bis(2-thienyl)-2,5-bis-[(cyclohexylmethyl)oxy]phenylene (P6). Ferric chloride (0.85 mmol) and 200 mL of $CHCl_3$ were refluxed for 2 h and cooled. 1,4-Bis(2-thienyl)-2,5-bis[(cyclohexylmethyl)oxy]benzene (**6**, 0.21 mmol) was added dissolved in 75 mL of $CHCl_3$. The mixture was refluxed for 72 h. The reaction medium was concentrated and the product precipitated into cold methanol. A dark red powder was collected by filtration and subsequently compensated by reaction with 30 mL of concentrated ammonium hydroxide. The product was washed with methanol and water and subsequently vacuum dried to yield the brick red neutral polymer. Anal. Calcd for $C_{28}H_{32}O_2S_2$: C, 72.06; H, 7.34; S, 13.74. Found: C, 63.89; H, 6.84; S, 9.62; Cl, 1.78.

Electrochemical and Spectroscopic Methods. Cyclic voltammetry (CV) was conducted utilizing platinum working and counter electrodes and a Ag/Ag^+ reference electrode. Potentials were controlled using an EG&G PAR Model 273 potentiostat/galvanostat. Polymer films for optoelectrochemical measurements were prepared on ITO-coated glass slides (Delta Technologies) as the working electrode. Electrolytes employed were 0.1 M tetrabutylammonium perchlorate (TBAP) in CH_3CN or CH_2Cl_2 (distilled over P_2O_5 prior to use). Electronic spectra were obtained using a Varian Cary 5E UV/vis/NIR spectrophotometer. Experimental details have been presented previously.[6d] In situ EPR measurements were carried out in an electrochemical EPR cell (Wilmad Glass) using a Bruker 200 EPR according to previously published methods.[6c] Spin concentrations were determined using DPPH (Aldrich) as a standard.[12] Mass changes at gold working electrodes (Valpey-Fisher) were monitored using an electrochemical quartz crystal microbalance (EQCM) as described previously.[13]

Results and Discussion

Chemically Prepared Poly[1,4-bis(2-thienyl)-2,5-bis[(cyclohexylmethyl)oxy]phenylene] (P6). The $FeCl_3$-induced oxidative polymerization of **6** followed by compensation with aqueous NH_3 yielded a brick-red neutral polymer that was totally insoluble. TGA showed the polymer to be stable to ca. 300 °C and was amorphous as determined by X-ray diffraction. FTIR studies indicated the disappearance of the α C−H stretching of the thiophene moiety with retention of the β C−H as expected for the formation of a conjugated polymer. Elemental analyses showed the product to be relatively impure and difficult to purify due to its insolubililty. While it is evident that **6** polymerizes under these oxidative conditions, this insolubility precluded proper structural analysis and study of electroactivity. As such, electrochemical methods were employed for polymerization and characterization.

Electropolymerization. All of the monomers studied in this series (**1**−**11**) can be oxidatively polymerized using electrochemical methods to yield electrically conducting polymers. Increasing the length of the alkoxy substituents (e.g., $OC_{12}H_{25}$, $OC_{16}H_{33}$, and $OC_{20}H_{41}$) causes the oxidized form of the oligomers to be relatively

Table 1. Electrochemical Results for Monomers and Polymers Obtained by Cyclic Voltammetry

monomer	$E_{p,m}$ (V)[a]	$E_{a,p}$ (V)	$E_{c,p}$ (V)	$E_{1/2}$ (V)
1	0.91	>1.0	0.82	
2	0.96	>1.1	0.97	
3	0.71	0.64	0.20, 0.58	0.27, 0.68
4	0.67	0.30, 0.65	0.25, 0.68	0.27, 0.68
5	0.67	0.40, 0.68	0.20, 0.61	0.30, 0.65
6	0.80	0.39, 0.62[a]	0.35, 0.55[a]	0.37, 0.60
7	0.78	0.62	0.50	0.56
8	0.76	0.61	0.50	0.55
9	0.65	0.50	0.46	0.48
10	0.65	0.14, 0.43	0.06, 0.43	0.10, 0.43
11	0.65	0.50	0.46	0.48

[a] All potentials reported vs Ag/Ag^+.

soluble and ineffective deposition occurs during electropolymerization. During anodic scanning of an electropolymerizable monomer solution in an electrolyte, a large irreversible current response is observed, indicating the formation and coupling of cation radicals.

The potential of the peak for the monomer oxidation ($E_{p,m}$) is dependent on the substituents as seen in Table 1. The increased electron donating ability of the alkoxy groups (relative to alkyl groups or unsubstituted monomer) results in a reduction of the monomer oxidation potential by ca. 100−200 mV depending on the heterocycle used. The higher oxidation potential observed with alkyl substitution in the thienyl derivatives, relative to the furanyl series, is due to the larger size of sulfur, compared to oxygen. This results in a greater steric interaction between the methyl group and the heterocycle.

Cyclic voltammetric (CV) scanning electropolymerization of these BHP monomers is generally characterized by the observation of polymer cathodic processes during the reverse scan. Multiple scans up to, or slightly beyond, $E_{p,m}$ then yields CVs where both the anodic and cathodic polymer redox processes grow in at potentials significantly lower than $E_{p,m}$. In contrast, the bis[(cyclohexylmethyl)oxy]-substituted monomer (**6**) exhibits a different behavior. Scanning to 0.9 V (Figure 1a) results in an $E_{p,m}$ at 0.8 V similar in nature to the other BHP systems investigated. Repeated scanning, however, shows a very slow film growth under these conditions. Extending the anodic scan to 1.1 V (Figure 1b) reveals a second oxidation ($E_{2,m}$) with an onset at 1.0 V. Repeated scanning under these conditions leads to the rapid development of cathodic processes ($E_{c2,p}$ and $E_{c1,p}$) at 0.55 and 0.35 V, along with an anodic process ($E_{a,p}$) at 0.5 V. During this excursion to higher potential, rapid electroactive film growth is observed.

The slow growth behavior can be attributed to the solubility of oxidized oligomers which form at low potentials, where the coupling products diffuse away from the electrode surface preventing formation of polymer on the electrode surface. As noted earlier, this phenomenon was observed for the highly soluble PBHP derivatives with the longest alkoxy substituents where the solubility of the oligomers precluded electrochemical polymerization.[6b] The second oxidation of **6** results in rapid electroactive film deposition. It is possible that this second process is due to the reaction of a coupled product to form a new cation radical. Since the result of this oxidation is rapid coupling, cross-linking of the polymer as it forms is likely.

To examine the potential dependence of this deposition further, the EQCM was used by monitoring the mass change during electropolymerization of **6** as shown in Figure 2. Scanning to 0.9 V results in a frequency decrease (mass increase) as expected for electropolym-

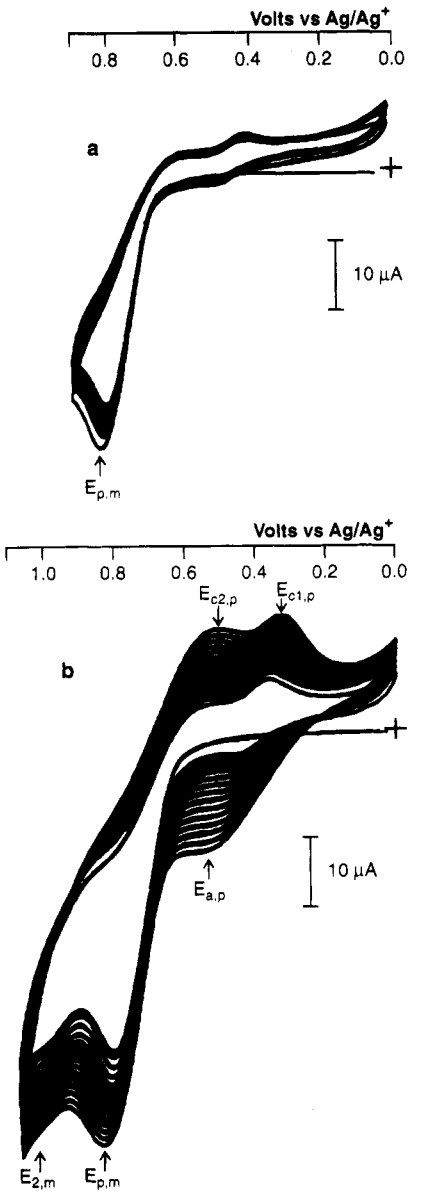

Figure 1. Multiple CV scan electropolymerization of 1,4-bis-(2-thienyl)-2,5-bis[(cyclohexylmethyl)oxy]benzene (**6**) in 0.1 M TBAP/CH_3CN with scanning to (a) +0.9 V and (b) +1.1 V.

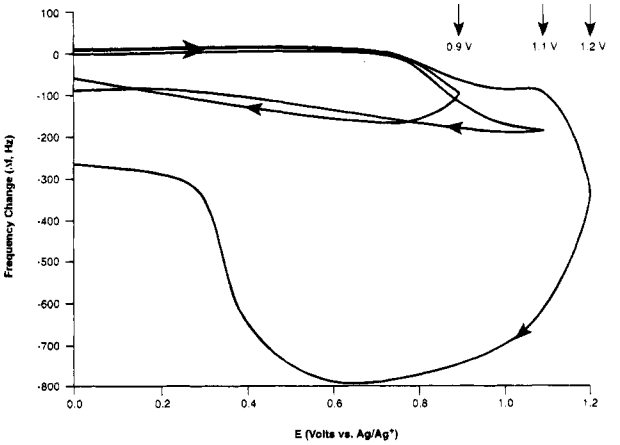

Figure 2. EQCM monitored frequency shifts during deposition of poly[1,4-bis(2-thienyl)-2,5-bis[(cyclohexylmethyl)oxy]-phenylene] (**P6**) from 0.1 M TBAP/CH_3CN with varied switching potentials.

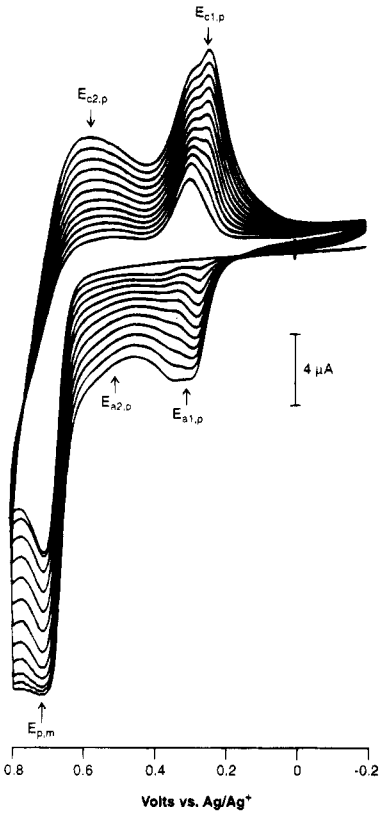

Figure 3. Multiple CV electropolymerization of 1,4-bis(2-thienyl)-2-heptoxy-5-methoxybenzene (**4**) in 0.1 M TBAP/CH_3CN with scanning to +0.8 V.

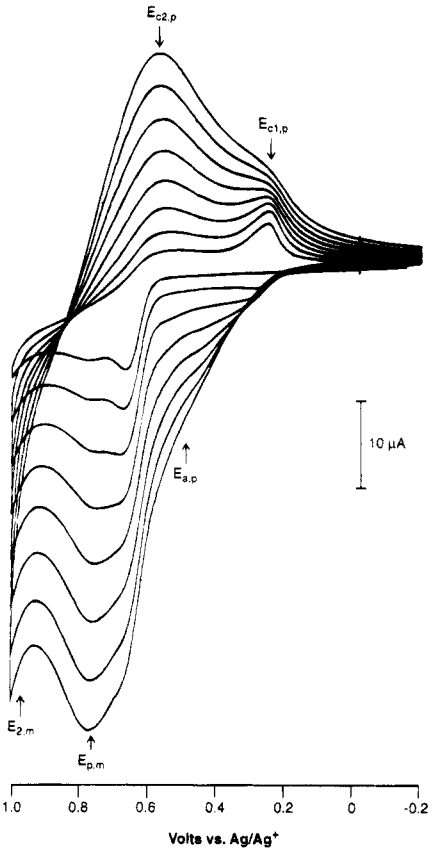

Figure 4. Multiple CV electropolymerization of 1,4-bis(2-thienyl)-2-heptoxy-5-methoxybenzene (**4**) in 0.1 M TBAP/CH_3CN with scanning to +1.0 V.

erization. During the return scan, the frequency increases as the polymer formed dedopes and anions are lost. A small net frequency change is observed at 0.0 V indicating that a small amount of polymer has permanently adhered to the electrode surface during this initial scan. Scanning with a switching potential change of +1.1 V, a plateau is observed in the frequency change as deposition occurs at a relatively slow rate on the polymer-covered electrode. Again the reverse scan shows a small irreversible mass change as a small amount of polymer deposition has occurred. Scanning beyond the second oxidation to 1.2 V results in a significantly larger frequency decrease and rapid mass deposition as electroactive polymer forms on the working electrode. The return scan shows a frequency increase, again indicative of the expulsion of counterions during polymer reduction, but the larger net mass increase at 0.0 V indicates a significant amount of polymer has deposited during this single scan.

By examining electropolymerizable BHPs with well-behaved polymerization characteristics at $E_{p,m}$, we find that this second redox process is found not only in **6** but in other monomers as well. As an example, Figure 3 shows the well-behaved electropolymerization of the methoxy/heptoxy-substituted bis(2-thienyl) monomer (**4**) with scanning to +0.8 V. Repeated scanning leads to the development of two polymer cathodic ($E_{c1,p}$ and $E_{c2,p}$) and anodic ($E_{a1,p}$ and $E_{a2,p}$) processes as electrically conductive and electroactive polymer deposits onto the working electrode surface. The electropolymerization behavior of **4** with scanning to +1.0 V is shown in Figure 4. The second oxidation ($E_{2,m}$) is now evident, and there are distinct changes in the electroactivity of the polymer. With scanning to $E_{p,m}$ (Figure 3) two anodic processes were visible, one as a distinct peak at +0.3 V and the other as a shoulder at +0.5 V. Scanning to higher potential during electropolymerization eliminates the peak $E_{a1,p}$, and all anodic redox activity is found at higher potential. The upper limit of the polymerization potential also has an impact on the polymer's cathodic redox processes. While scanning to $E_{p,m}$ yields two distinct cathodic processes and a higher peak current for $E_{c1,p}$ compared to $E_{c2,p}$, scanning to higher potential increases the relative current for $E_{c2,p}$. At the same time, there is a general broadening of the peaks and loss of resolution.

Polymer Cyclic Voltammetry. Following a scanning electropolymerization up to $E_{p,m}$ of **1**, **3**, and **4**, polymer films **P1**, **P3**, and **P4** were rinsed with CH_3CN, and their redox processes examined in monomer-free 0.1 M TBAP/CH_3CN electrolyte by CV. Figure 5 shows the CV behavior of these polymers and the redox results for all polymers prepared under similar conditions are summarized in Table 1. The magnitude of the peak current (i_p) scales linearly with the scan rate in all cases which indicates that the electroactive species are electrode bound. The oxidation potentials of the polymers follow a trend similar to that observed for the monomers due to the electronic and steric effects discussed earlier. In both the thiophene and furan series containing long-chain alkoxy substituents, a well-resolved low-potential redox couple is observed in addition to the major broad process at higher potential. This is illustrated by the inclusion of an heptoxy side chain as shown in Figure 5c. We attribute the presence of these two redox couples to the separation of the neutral-to-polaron and polaron-to-bipolaron charge-carrier formation events based on previous in situ EPR studies.[6c] This behavior has been observed previously in poly(3-alkylthiophenes), where the extent of separa-

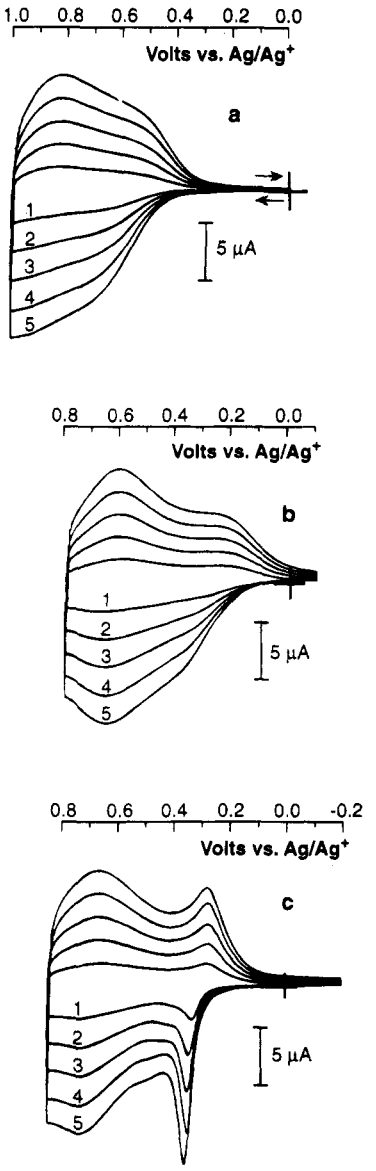

Figure 5. Cyclic voltammograms in monomer-free 0.1 M TBAP/CH_3CN electrolyte for (a) poly[1,4-bis(2-thienyl)phenylene] (**P1**), (b) poly[1,4-bis(2-thienyl)-2,5-dimethoxyphenylene] (**P3**), and (c) poly[1,4-bis(2-thienyl)-2-heptoxy-5-methoxyphenylene] (**P4**) electrosynthesized by scanning to $E_{p,m}$ carried out as a function of scan rate: (1) 25, (2) 50, (3) 75, (4) 100, (5) 125 mV/s.

tion depends on the length of the alkyl chain,[10] and in alkoxy-substituted polythiophenes.[9]

The separation of the redox processes is more pronounced in the long-chain substituted derivatives and, since the heptoxy groups exert a similar electron-donating effect as methoxy groups, this suggests a morphology component to this phenomenon. The decreased monomer oxidation potential of the alkoxy-substituted monomers leads to polymers with a lower degree of cross-linking and β-coupling and, likely, a higher degree of swelling in the switching electrolyte. For example, the cyclic voltammogram of polythiophene, electrosynthesized from bithiophene, displays two cathodic current responses, whereas the higher monomer oxidation potential of thiophene leads to films with a single redox couple.[14] Noting the CV switching potential effect on the polymer's redox processes of **P4** during film growth illustrated in Figures 3 and 4, we compare the electroactivity of **P4** prepared with varied switching potentials in monomer-free electrolyte. Figure 6 shows

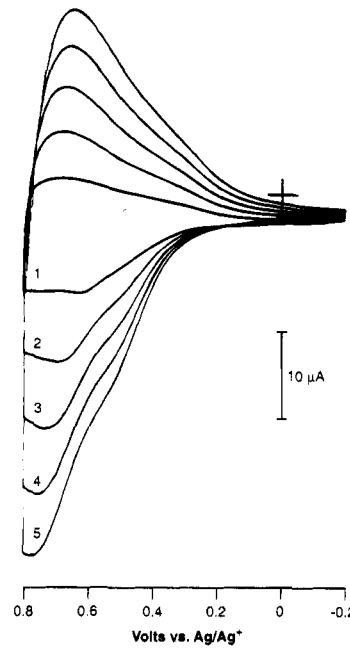

Figure 6. Cyclic voltammograms of poly[1,4-bis(2-thienyl)-2-heptoxy-5-methoxyphenylene] (**P4**), electrosynthesized by scanning to +1.1 V, carried out as a function of scan rate: (1) 25, (2) 50, (3) 75, (4) 100, and (5) 125 mV/s.

the CV for **P4** prepared with a switching potential of +1.1 V for direct comparison to Figure 5c. It is evident that carrying the polymerization out by repeated scanning to the higher potential redox process has drastically altered the polymer's electroactivity with almost complete elimination of the low-potential process ($E_{a1,p}$ and $E_{c1,p}$). The chemistry occurring at this high potential limits the electroactivity by producing a polymer which is highly cross-linked, thereby inhibiting counterion mobility. An overall decrease in electroactivity is observed which may be due to trapped sites which become isolated and inaccessible to counterion transport. We find the electrochemical response of **P4**, prepared under these high-potential switching conditions, to be similar to the poorly conducting methyl-substituted thienyl derivative **P2**.

To examine this effect of the high switching potential further, the (cyclohexylmethyl)oxy-substituted monomer, **6**, was polymerized by repeated scanning to +1.1 V, and its CV response measured in CH_2Cl_2 and CH_3CN as shown in Figure 7. The CV of the polymer lacks the first, low-potential couple when cycled in CH_3CN (Figure 7b) but displays two couples in CH_2Cl_2 (Figure 7a). The linear alkoxy-substituted polymers are more highly soluble in CH_2Cl_2 compared to CH_3CN, suggesting it more effectively swells the insoluble cyclohexylmethyloxy polymer and facilitates counterion insertion.

The above results suggest that the energy required for counterion insertion is an important factor in determining the stability of intermediate charge carriers.[14] The potential necessary to insert counterions into films of unsubstituted, alkyl-substituted or cross-linked polymers is greater than or equal to the potential for bipolaron formation; therefore, a single two-electron oxidation results. The polymers which exhibit two couples allow facile counterion movement due to the low oxidation potentials of their monomers (resulting in minimal cross-linking during electropolymerization at $E_{p,m}$) and solvation effects induced by long side chains.

Two electrochemical properties support the suggestion that polarons are formed at the first redox couple of

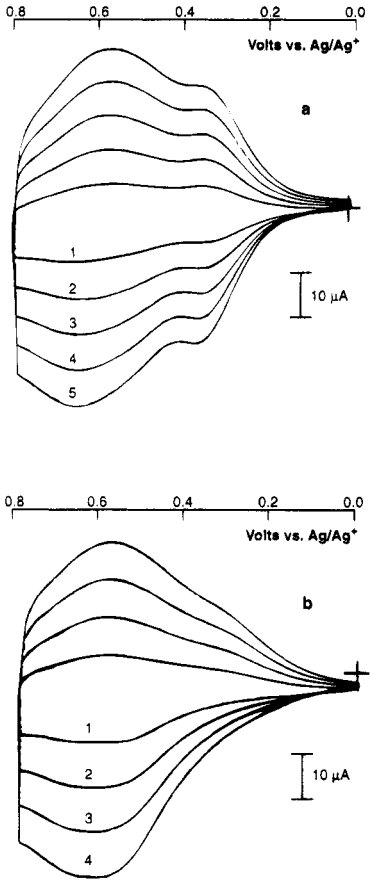

Figure 7. Cyclic voltammograms of poly[1,4-bis(2-thienyl)-2,5-bis[(cyclohexylmethyl)oxy]phenylene] (**P6**) electrosynthesized by scanning to +1.1 V and switched in monomer-free 0.1 M TBAP in (a) CH_2Cl_2 and (b) CH_3CN as a function of scan rate: (1) 25, (2) 50, (3) 75, (4) 100, and (5) 125 mV/s.

these polymers. First, the peak widths of the first couple are narrow with respect to the second couple. Several polythiophene derivatives containing ether groups at the 3 position have been shown to display two distinct redox couples in their CVs, and the presence of a relatively sharp initial couple is characteristic of these systems.[9] The width of current responses in the cyclic voltammograms of surface bound species is ideally a constant value of $90.6/n$ mV, where n is the number of electrons transferred. Larger values are indicative of repulsive interactions within the film.[15] Because polarons possess only a single charge and bipolarons contain two positive charges, repulsive interactions are expected to cause a larger peak-broadening effect in the formation of bipolarons. The narrow current responses in the low-potential couple of these systems suggests that monovalent charge carriers rather than dicationic carriers are present. Secondly, the peak separation of the second couple is slightly smaller in the polymers with two couples than in the polymers which undergo a single, two-electron process. The large-peak separation traditionally observed in conducting polymers has been ascribed to the large differences in conductivity between the oxidized and reduced states.[15] In those polymers where intermediate charge carriers (polarons) are formed at a lower potential the conductivity difference before and after the second oxidation is greatly reduced, resulting in a near-zero separation between the anodic and cathodic current responses for the second couple.

EPR Electrochemistry. The presence of spin-bearing polaron charge carriers at intermediate doping

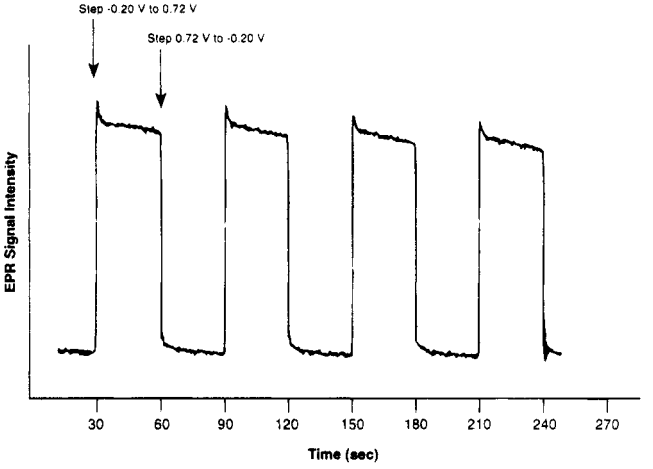

Figure 8. Temporal dependence of the EPR signal intensity for poly[1,4-bis(2-furanyl)-2,5-diheptoxyphenylene] (**P11**) during repeated potential steps between −0.2 V (neutral) and +0.72 V (intermediate oxidation state) in 0.1 M TBAP/CH_3CN.

levels have been further confirmed by investigating the EPR signal of these polymers as a function of applied potential. In studies of poly[1,4-bis(2-thienyl)-2,5-diheptoxyphenylene] (**P5**), we have previously reported that the maximum spin concentration is at a potential between the redox processes observed by cyclic voltammetry.[6c] This indicates that spin-bearing polarons are formed at the first redox couple and converted into diamagnetic bipolarons at the second couple. Polymers which display only a single redox couple show no evidence of paramagnetism at any potential, indicating that the neutral polymer is oxidized directly to the diamagnetic bipolaron, or that the lifetime of the paramagnetic species is shorter than the time scale of the experiment.

The stability of the intermediate charge carriers formed on polymers with sufficiently long substituents has been investigated by monitoring the EPR signal during potential stepping. As an example, Figure 8 shows the EPR response with repeated stepping of the potential from a neutral value (−0.20 V) to a potential between the two redox processes (+0.72 V) and back to the neutral state for poly[1,4-bis(2-furanyl)-2,5-diheptoxyphenylene] (**P11**). After an immediate and large increase in the EPR signal, a small, rapid decay is observed which may be due to the coupling of adjacent polarons into a bipolaron and a neutral site. After this initial decay, the signal remains relatively constant. Returning the potential to −0.20 V results in a loss of the EPR signal as the polymer is returned to the neutral state. Subsequent stepping of the potential between +0.72 and +1.20 V results in a rapid decrease in the EPR signal as polarons are converted to bipolarons at the high potential, followed by a return of the paramagnetism at +0.72 V. Both of these redox processes, neutral to polaron and polaron to bipolaron, are reproducible for many cycles. At approximately 1.20 V, 10% of the EPR signal remains, suggesting that some polarons are trapped and are unable to couple or become fully oxidized. The EPR signal could be reduced to zero by stepping the potential to >1.50 V, but this results in an irreversible loss of electroactivity as the polymer becomes overoxidized.

Utilizing a DPPH spin standard, the concentration of spins has been determined for both **P5** and **P11** held at the potential of maximum EPR signal. Paramagnet-

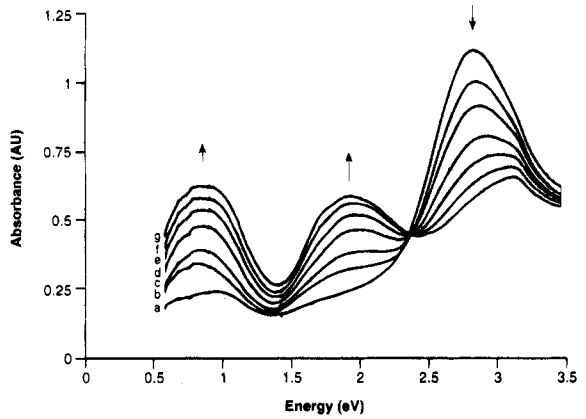

Figure 9. Potential dependence of the optical absorption for poly[1,4-bis(2-thienyl)-2,5-bis[(cyclohexylmethyl)oxy]phenylene] (**P6**) equilibrated in 0.1 M TBAP/CH_3CN at (a) 0.0, (b) 0.60, (c) 0.70, (d) 0.80, (e) 0.90, (f) 0.95, and (g) 1.00 V.

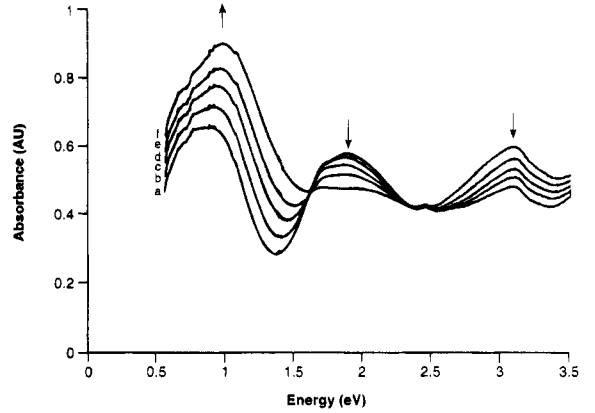

Figure 10. Potential dependence of the optical absorption for poly[1,4-bis(2-thienyl)-2,5-bis[(cyclohexylmethyl)oxy]phenylene] (**P6**) equilibrated in 0.1 M TBAP/CH_3CN at (a) 1.05, (b) 1.10, (c) 1.15, (d) 1.20, (e) 1.25, and (f) 1.30 V.

ism levels of 0.25 and 0.10 spins/repeat unit (one spin per 12 and one spin per 30 rings) for the thiophene and furan polymer respectively have been observed. This value is approximately an order of magnitude higher than that observed previously for polythiophene (electrosynthesized from bithiophene)[16] and supports the stabilizing effects of long-chain alkoxy pendants on polaron-charge carriers.

Optoelectrochemistry. The electronic band structure of this polymer series has been investigated using optoelectrochemistry. The electronic bandgaps (E_g), determined from the onset of π to π^* transition, follow the trend expected considering the electronic and steric effects discussed above. The band gap for the unsubstituted thiophene polymer **P1** is 2.3 eV, which is increased to 2.6 eV with the methyl substitution in **P2**. Alkoxy substitution lowers the energy gap to 2.1 eV for **P3-P6**. A similar trend is observed for E_g for the unsubstituted, methyl-substituted, and methoxy-substituted furan polymers (2.3, 2.4, 2.2 eV, respectively) with the expected smaller difference for alkyl substitution due to the smaller effects of steric hindrance.

Upon electrochemical doping, new transitions are observed and intragap electronic levels are created during charge-carrier generation, as illustrated in Figure 9 for poly[1,4-bis(2-thienyl)-2,5-bis[(cyclohexylmethyl)oxy]phenylene] (**P6**). This behavior is commonly observed in conducting polymers with nondegenerate ground states.[5d,17] In Figure 9, the electrode potential is stepped anodically a small amount and a spectrum recorded at each potential up to 1.0 V. At each subsequent doping level the absorption intensity increases for the low-energy transitions and decreases for the high-energy intergap transition, indicating increasing charge carrier concentration. Each of the polymers in this series exhibits similar behavior. The alkoxy-substituted polymers undergo a further change in the nature of their charge carriers at potentials just below their breakdown voltage. This change is illustrated in Figure 10 for the identical film used in Figure 9 as the potential is incrementally stepped from +1.0 to +1.3 V. In the case of **P6** at these high doping levels, the peak attributed to the transition between the valence band and the higher energy intragap state decreases in intensity, while the energy of the lowest energy transition shifts to higher energies.

This evolution of the optical spectra can be illustrated by the band-structure diagram in Figure 11. In the neutral form, the polymer exhibits a simple π to π^* transition with an onset energy at E_g as shown in Figure 11a. As the initial charge carriers are formed, likely a combination of polarons and bipolarons (Figure 11b and 11c), the midgap states are created at the expense of the highest energy states in the valence band. This causes a shift in the π to π^* transition to higher energy. Note that the λ_{max} for this transition in **P6** shifts from 2.7 to 3.1 eV during doping. At +1.0 V the polymer contains a high density of bipolarons which can be represented by bands (Figuer 11d) due to the large number of states possible, caused by effective conjugation lengths in the material. At the higher potentials ($+1.0\ V \leq E \leq +1.3\ V$) the change in the optical spectra can be attributed to the formation of metallic-like charge carriers.[17] The intragap bipolaron bands become sufficiently broad at high doping levels that they intersect with the valence and conduction bands as illustrated in Figure 11e. In our series, this behavior is observed only in the alkoxy-substituted derivatives of both heterocycles. At potentials above 1.5 V, each of the polymers undergoes an irreversible degradation due to overoxidation, resulting in a pronounced decrease in electroactivity.[18]

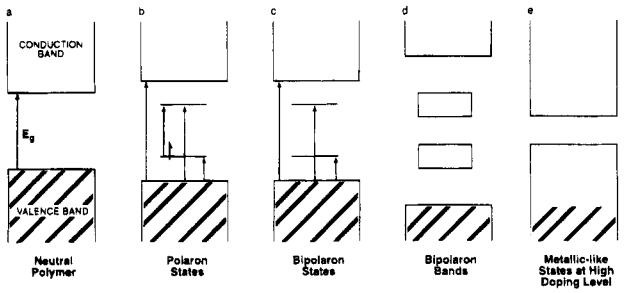

Figure 11. Electronic band diagram for nondegenerate ground-state conjugated polymers showing (a) neutral state, (b) polaron states, (c) bipolaron states, (d) bipolaron bands, and (e) metallic-like bands.

The presence of metallic charge carriers in these systems, and their absence in others, can be explained by comparing the monomer and polymer oxidation potentials. Since overoxidation of these conducting polymers involves irreversible structural changes in the polymer backbone,[18] the effect of pendant substituents on the potential for overoxidation will be minimal. Pendant groups have a pronounced effect on the polymer's initial oxidation potential, however, as shown in Table 1. Due to both the electron-donating nature of their substituents and a morphology more conducive to counterion transport, the alkoxy-substituted polymers

display a significantly lower oxidation potential. At voltages above 1.0 V, the doping levels for these polymers are significantly higher than for the methyl-substituted and unsubstituted derivatives. In addition to the low oxidation potentials, the long-chain alkoxy-substituted derivatives are able to accommodate a larger number of counterions due to their morphology. The doping levels in the furanyl series have been shown to increase dramatically with the length of the alkoxy chain and reach a level of 0.40 dopants/monomer unit in the diheptoxy-substituted polymer **P11**.[6d]

Conclusions

The types and stability of charge carriers in a series of substituted poly[1,4-bis(2-heterocycle)phenylenes] have been found to be highly substituent dependent. Alkoxy substitution, through a combination of electron-donating and steric factors, results in a marked decrease in monomer and polymer oxidation potentials and a decrease in the optical bandgap. Substitution with long-chain alkoxy groups results in the formation of stable paramagnetic charge carriers at intermediate doping levels, and metallic charge carriers at high doping levels.

Acknowledgment. This work was supported by grants from the Air Force Office of Scientific Research (F49620-92-J-0509), the National Science Foundation (CHE 9307732), and the Naval Air Warfare Center.

References and Notes

(1) Permanent address: Milliken Research Corp., Post Office Box 1927, M-405, Spartanburg, SC 29304.
(2) Reynolds, J. R.; Pomerantz, M. P. In *Electroresponsive Molecular and Polymeric Systems*; Marcel Dekker, Inc.: New York, 1991; p 187 (see for a comprehensive review).
(3) (a) Ruhe, J.; Ezquerra, T.; Wegner, G. *Makromol. Chem., Rapid Commun.* **1989**, *10*, 103. (b) Martina, S.; Schlüter, A.-D. *Macromolecules* **1992**, *25*, 3607.
(4) (a) Rehahn, M.; Schlüter, A.-D.; Wegner, G.; Feast, W. J. *Polymer* **1989**, *10*, 1060. (b) Rehahn, M.; Schlüter, A.-D.; Wegner, G. *Makromol. Chem.* **1990**, *191*, 1991.
(5) (a) Patil, A. O.; Ikenoue, Y.; Wudl, F.; Heeger, A. J. *J. Am. Chem. Soc.* **1987**, *109*, 1858. (b) Patil, A. O.; Ikenoue, Y.; Basecu, H.; Colaneri, H.; Chen, J.; Wudl, F.; Heeger, A. J. *Synth. Met.* **1987**, *20*, 151. (c) Reynolds, J. R.; Sundaresan, N. S.; Pomerantz, M.; Basak, S.; Baker, C. K. *J. Electroanal. Chem.* **1988**, *250*, 355. (d) Child, A. D.; Reynolds, J. R. *Macromolecules* **1994**, *27*, 1975.
(6) (a) Reynolds, J. R.; Ruiz, J. P.; Child, A. D.; Nayak, K.; Marynick, D. S. *Macromolecules* **1991**, *24*, 678. (b) Ruiz, J. P.; Dharia, J. R.; Reynolds, J. R.; Buckley, L. F. *Macromolecules* **1992**, *25*, 849. (c) Child, A. D.; Reynolds, J. R. *J. Chem. Soc., Chem. Commun.* **1991**, 1779. (d) Reynolds, J. R.; Child, A. D.; Ruiz, J. P.; Hong, S. Y.; Marynick, D. S. *Macromolecules* **1993**, *26*, 2095.
(7) (a) Danieli, R.; Ostoja, R.; Tiecco, M.; Zamboni, R.; Taliani, C. *J. Chem. Soc., Chem. Commun.* **1986**, 1473. (b) Mitsuhara, T.; Tanaka, S.; Kaeriyama, K. *J. Chem. Soc., Chem. Commun.* **1987**, 743. (c) Pelter, A.; Maud, J. M.; Jenkins, I.; Sadeka, C.; Coles, G. *Tetrahedron Lett.* **1989**, *30*, 3461.
(8) Hong, S. Y.; Marynick, D. S. *Macromolecules* **1992**, *25*, 3591.
(9) (a) Leclerc, M.; Diaz, F. M.; Wegner, G. *Makromol. Chem.* **1989**, *190*, 3105. (b) Kaeriyama, K.; Tanaka, S.; Sato, M.; Hamada, M. *Synth. Met.* **1989**, *28*, C611. (c) Elsenbaumer, R. L.; Jen, K. Y.; Miller, G. G.; Shacklette, L. W. *Synth. Met.* **1987**, *18*, 277. (d) Roncali, J.; Shi, L. H.; Garreau, R.; Garnier, F.; Lemaire, M. *Synth. Met.* **1990**, *36*, 267.
(10) Roncali, J.; Garreau, R.; Yassar, A.; Marque, P.; Garnier, F.; Lemaire, M. *J. Phys. Chem.* **1987**, *91*, 6706.
(11) Zotti, G.; Schiavon, G.; Berlin, A.; Pagani, G. *Chem. Mater.* **1993**, *5*, 620.
(12) Lothe, J.; Eia, G. *Acta Chem. Scand.* **1958**, *12*, 1535.
(13) Baker, C. K.; Reynolds, J. R. *J. Electroanal. Chem.* **1988**, *251*, 307.
(14) Zotti, G.; Schiavon, G. *Synth. Met.* **1989**, *31*, 347.
(15) Abruna, H. *Coord. Chem. Rev.* **1988**, *86*, 135.
(16) Hoier, S. N.; Park, S.-M. *J. Phys. Chem.* **1992**, *96*, 5188.
(17) (a) Chung, T. C.; Kaufman, J. H.; Heeger, A. J.; Wudl, F. *Phys. Rev. B: Condens. Matter* **1984**, *30*, 702. (b) Bredas, J. L.; Themans, B.; Fripiat, J. G.; Andre, J. M.; Chance, R. R. *Phys. Rev. B: Condens. Matter* **1984**, *29*, 6761. (c) Bredas, J. L.; Street, G. B. *Acc. Chem. Res.* **1985**, *18*, 309. (d) Sun, Z.; Frank, A. J. *J. Chem. Phys.* **1991**, *94*, 4600.
(18) Tsai, E. W.; Basak, S.; Ruiz, J. P.; Reynolds, J. R.; Rajeshwar, K. *J. Electrochem. Soc.* **1989**, *136*, 3683.

MA950469S